

Original Article

A novel strontium-loaded silk fibroin nanofibrous membrane for guided bone regeneration: in vitro and in vivo studies

Shijun Lu^{1,2*}, Ming Shen^{3*}, Feng Zhang⁴, Peng Wang⁵, Baoqi Zuo⁵, Xichao Zhou⁶, Xinran You⁷, Zhendong Wang³, Hongchen Liu¹

¹Institute of Stomatology, Chinese People Liberation Army General Hospital, Beijing, China; ²Department of Stomatology, Suzhou Health College, Suzhou, China; ³Jiangsu Key Laboratory of Oral Diseases, Affiliated Hospital of Stomatology, Nanjing Medical University, Nanjing, China; ⁴Jiangsu Province Key Laboratory of Stem Cell Research, Medical College, Soochow University, Suzhou, China; ⁵National Engineering Laboratory for Modern Silk, College of Textile and Clothing Engineering, Soochow University, Suzhou, China; ⁶Department of Orthopedics, The First Affiliated Hospital of Soochow University, Suzhou, China; ⁷Affiliated Suzhou Hospital of Nanjing Medical University, Suzhou, China. *Equal contributors.

Received November 17, 2015; Accepted January 25, 2016; Epub April 15, 2016; Published April 30, 2016

Abstract: The silk fibroin (SF) nanofibrous membrane is a good candidate for clinical application in bone and periodontal regenerative therapy. Strontium (Sr), as a natural element in human bone, can hinder osteoclast activity and promote bone formation. This study aims to evaluate in vitro and in vivo the feasibility of strontium-loaded silk fibroin nanofibrous membrane (Sr-SFM) for guided bone regeneration (GBR). The Sr-SFM was fabricated by electrospinning, and the structure characteristics and strontium ion release pattern were analyzed. To examine the biocompatibility of Sr-SFM, we investigated cell morphology, proliferation and differentiation. The GBR efficacy of Sr-SFM was evaluated in rat calvarial defects. The Sr-SFM exhibited uniform nanofibrous structure and a sustained release of strontium over a 14-day period. In vitro tests, the cell numbers and ALP activities of rBMSCs cultured in Sr-SFMs were significantly higher than that in pure SFM. In vivo test at 6 weeks, both micro-CT and histological analyses showed that the Sr-SFM group got significantly greater bone formation than pure SFM or uncovered groups. In conclusion, the Sr-SFMs developed in this study showed long-term release of Sr²⁺, improved cell proliferation and osteogenic differentiation of hMSCs in vitro, and increased new bone formation in vivo, strongly suggesting their potential application towards GBR.

Keywords: Silk fibroinnanofiber, strontium, drug release, guided bone regeneration, rat calvarial defects

Introduction

Guided bone regeneration (GBR) is a widely used strategy to preserve and reconstruct alveolar bony defects. The GBR technique uses a membrane, which serves as a barrier to resist the fast growing epithelial and connective tissue migration into the bony defect. Meanwhile the membrane maintains a secluded space to allow the necessary time for osteogenic cell proliferation and new bone formation [1]. The ideal GBR membrane needs to satisfy the following criteria such as biocompatibility, space creation and maintenance, ability to exclude epithelial and connective tissue, osteogenesis,

proper degradation rate, clinical manageability and cost-effectiveness [2].

In general, there are two types of GBR membranes materials: resorbable and non-resorbable, according to their degradation characteristics. The non-resorbable membranes (e.g. expanded polytetrafluoroethylene, e-PTFE) have a desirable correlation between the level of bone regeneration and space maintenance. However, they need a secondary surgical procedure for membrane removal, which may result in additional discomfort, infection, and increased economic burden [3]. In order to overcome these problems, all kinds of resorbable mem-

Strontium-loaded silk fibroin guided bone regeneration

branes have been developed, and the main resorbable membrane in GBR technique is natural collagen membrane. They show well bone regenerative results due to their excellent biocompatibility and cell affinity. However, the collagen derived from animal sources may have problems such as disease transmission, increased cost, ethical and cultural issues. Moreover its low mechanical strength and variable degradation rate are a concern to many clinicians [4]. Because of these shortcomings or defects in currently used membranes, new composite biomaterials with better properties are required.

Silk fibroin (SF) is obtained from cocoons of Silkworm *Bombyx mori*, which has been used as a potential biomedical material for more than ten years [5]. SF has some favorable properties, such as good biocompatibility, oxygen and water vapor permeability, non-cytotoxicity, controllable biodegradability, high tensile strength, and non-inflammatory characteristics [6, 7]. Recently, SF nanofibrous membranes (SFMs) for guided bone regeneration had been developed by electrospinning technique. It can provide a biomimetic cellular environment by mimicking the dimensions of the extracellular matrix (ECM), which can improve osteoblastic cells function and bone regeneration [8]. Furthermore, because the pore size of the electrospun membranes is smaller than the average cell size, the membranes can inhibit cell penetration but allow efficient exchange of nutrients and metabolic wastes [9, 10]. However silk fibroins do not exert favorable biological activity to induce osteogenesis. Thus the current studies have attempted to develop a novel GBR membrane that not only as a barrier membrane, but also provide bioactive properties to stimulate bone regeneration in defect site [11-13].

Recently, the positive effects of strontium have been approved for the treatment of osteoporotic bone or bone defects [14-16]. Strontium was found to increase new bone formation by inducing osteoblast proliferation and differentiation. Meanwhile it was proved to reduce bone resorption by inhibiting osteoclast maturation [17, 18]. Since 2004, strontium ranelate (SrR) as a daily oral drug has been recommended for the treatment and prevention of osteoporosis. However, the bioavailability of SrR is relatively low and the actual concentration of stron-

tium at a specific bone-healing site cannot be measured and therefore remains unknown. Since high-dose administration of SrR is associated with the occurrence of diarrhea, headache and nausea [19], a local or targeted release system for strontium ions would be a better solution. Therefore several approaches have been used in order to stimulate bone formation, osseointegration, and also inhibit bone resorption through local administration of strontium ions, such as strontium modified calcium phosphate cement [15], strontium-substituted calcium silicate bioactive ceramics [20], strontium containing coated on implant surfaces [21, 22]. However, very few studies focused on the application of Sr-loading in GBR technique.

In the present study, the first introduction of Sr (in the forms of SrCl) into electrospun silk fibroin nanofibrous membrane was designed and achieved for GBR. The physical-chemical characterizations were performed in order to determine the effects of Sr-loading on the morphology, structure and properties of SFM. Rat bone-marrow stromal cells (rBMSCs) were cultured on Sr-SFM to evaluate the effect of Sr on the SFM properties related to biological responses, such as cell proliferation, differentiation. Finally, Sr-SFM was implanted into a rat calvarial defect to ascertain potential advantages of Sr-SFM for GBR.

Materials and methods

Preparation of SF nanofibrous membranes containing strontium (Sr-SFMs)

Bombyx mori cocoons were degummed three times with a 0.05 wt% Na₂CO₃ solution at 100°C for 50 min, and then rinsed thoroughly with distilled water to extract the sericin proteins. The dried degummed silk was then dissolved in LiBr-formic acid with LiBr concentration of 4% to prepare 8% (w/w) SF solutions. The solutions were poured into on the culture dish to get dried film after formic acid evaporation. The dried film was then rinsed with deionized water to desalt. Then, SF electrospin solution was prepared by dissolving degummed silk film in 98% formic acid (FA) containing 0, 1%, 5% and 10% SrCl₂ at a concentration of 8% w. This SF-SrCl₂-FA solution was used for electrospinning with the following electrospin parameters: needle spinneret diameter 0.42 mm,

Strontium-loaded silk fibroin guided bone regeneration

injection rate 1 ml/h, working distance 10 cm, and voltage 15 kV. After 20 h electrospinning preparation, 0.4 mm thickness SF nanofibrous membranes were obtained. For post-treatment, the electrospun SF nanofibers were put in 75% ethanol vapor for 1 h and then dried in air.

Thereafter, the Sr-SFMs were trimmed into disc sharp with 15 mm in diameter matching the size of 24-well plate for vitro tests. Meanwhile, the Sr-SFMs were also cut into 6 mm×6 mm squares for vivo tests. Finally, all the prepared Sr-SFMs were sterilized by gamma irradiation at standard dose of 25 kGy before experiments.

Characterization of Sr-SFMs

Scanning electron microscopy (SEM): The morphology of the prepared Sr-SFMs (0, 1, 5 and 10%) were observed using an SEM (Hitachi S-4800, Japan) at 20°C, 60 RH. Before being observed by SEM, these membranes were gold coated. The nanofiber diameter in each sample was calculated using Image-J software.

X-ray diffraction (XRD): The structure of the prepared Sr-SFMs (0, 1, 5 and 10%) were analyzed by X-ray diffractometer (X'Pert-Pro MPD, Panalytical B.V. Holland).

X-ray photoelectron spectroscopy (XPS): Chemical compositions of the prepared Sr-SFMs (1, 5 and 10%) were determined by SHIMADZU/KRATOS X-ray photoelectron spectrometer (XPS) to confirm the existence of Sr.

In vitro strontium release tests

The prepared Sr-SFMs (1, 5 and 10%) were placed in a 24-well cell culture plate (Sigma, USA), and then 1 ml phosphate buffer saline (PBS) (Sigma, USA) was added into each well at 37°C/5% CO₂ under static conditions. The total volume of PBS were collected and replaced with fresh PBS at 1 h, 6 h, 12 h, 1 d, 3 d, 7 d, 14 d. The amounts of strontium release in the collected PBS samples were measured using inductively coupled plasma-optical emission spectrometer (ICP-OES) (Thermo Fisher, USA). Each measurement was carried out in triplicate.

In vitro cell culture study

BMSCs isolation and culture: Rat bone marrow stromal cells (rBMSCs) were isolated and cul-

tured according to the previous published method [23]. Briefly, rBMSCs were isolated from the femora of 4-weeks-old male Sprague-Dawley rats and incubated in DMEM (Gibco, USA) supplemented with 10% fetal bovine serum (FBS) (Hyclone, USA), 100 U/ml streptomycin and 100 U/ml penicillin, and at 37°C in a humid atmosphere of 5% CO₂. After 24 hours, the non-adherent cells were rinsed away using PBS several times and the medium was refreshed every 2 or 3 days. Its passage was performed at 80% confluence by treatment with 0.25% trypsin/0.01% EDTA (Gibco, USA). rBMSCs in passage 3-4 were used for subsequent experiments.

Fluorescence-activated cell sorting (FACS) analysis: For phenotypic characterization analysis, cells were incubated for 30 min on ice with phycoerythrin (PE)-conjugated antibodies against CD45, CD73 and fluorescein isothiocyanate (FITC)-conjugated antibodies against CD34, CD90 (all from Boster, China). Analysis was performed by a flow cytometer (BD Accuri C6, BD Biosciences, Germany).

Proliferation of rBMSCs on Sr-SFMs: Cell Counting Kit-8 (CCK-8) (Dojindo Laboratories, Japan) assay was used to evaluate cellular proliferation on Sr-SFMs (0, 1, 5 and 10%; three membranes per group). Briefly, 1×10⁴ rBMSCs in 1ml medium were seeded onto each membrane, which were incubated at 37°C in a humid air of 5% CO₂. The analysis was performed at days 1, 3, 5 and 7 under manufacturer's instruction. Measurement was done at 450 nm using a micro-plate reader (μQuant, Biotek, USA).

Morphology of rBMSCs on Sr-SFMs: In order to observe the morphology of rBMSCs on Sr-SFMs (0, 1, 5 and 10%), we seeded 1×10⁴ rBMSCs onto each membrane in a 24-well plate. After culturing for 1 and 7 days, all the samples were fixed with 4% paraformaldehyde (Sigma, USA) and 3% glutaraldehyde (Sigma, USA) overnight, washed in PBS for 15 min, dehydrated in a graded ethanol (50, 60, 70, 90, 95 and 100% (v/v)), and dried in hexamethyldisilazane. Finally, samples were coated with gold, and observed by SEM.

Alkaline phosphatase (ALP) activity of rBMSCs on Sr-SFMs: For osteogenic differentiation, the cells were cultured in osteogenic medium. It

Strontium-loaded silk fibroin guided bone regeneration

was composed of DMEM supplemented with 0.1 μ M dexamethasone, 50 μ g/ml ascorbic acid and 10 mM β -glycerophosphate (all from Sigma, USA). After cells cultured on Sr-SFMs (0, 1, 5 and 10%; three membranes per group) for 7 and 14 days, the ALP activity, a marker of osteoblast differentiation, was measured using Alkaline Phosphatase Assay Kit (Beyotime, China) according to the manufacturer's instruction. The results were expressed as the OD value by an ELISA reader (Multiskan Spectrum, Thermo Fisher Scientific, USA) at a wavelength of 405 nm.

In vivo guided bone regeneration study

Animal surgery for rat calvarial defect model: This entire experimental protocol was approved by the Animal Care and Experiment Committee of Institute of Soochow University (Suzhou, China). Nine healthy male Sprague-Dawley rats with an average weight of 250 g were used in this experiment. The rats were randomly divided into three groups: (1) Sr-SFM; (2) SFM; (3) control group. Rats were general anesthetized and a longitudinal incision was made in skull from the nasal to occipital region. After separating the skin and muscle, the calvarial surface on both sides of midline were exposed. A dental-trephine bur (5 mm in diameter; Dentium, Korea) was used to create bilateral full-thickness calvarial defects under sterile saline irrigation (**Figure 1A**). Then calvarial defects were covered with Sr-SFMs, SFMs or left empty as negative control. The membranes were trimmed into rectangle (14 mm \times 7 mm in size) to fit well of the defects (**Figure 1B**). The pericranium and skin were sutured in layers with 3-0 silk sutures. After surgery, the rats were caged and received food and water individually. After 6 week healing, the animals were euthanized and the calvarial samples including the defects, the membranes and the surrounding tissue were removed from the bodies. These samples were fixed with 4% paraformaldehyde for 24 h at room temperature.

Micro-computed tomography analysis: The prepared samples were scanned by using a micro-CT (SkyScan 1176, Bruker-microCT, Kontich, Belgium). The scanning conditions were set at voltage 65 KV; current 100 μ A, exposure time 600 ms, and Al filter 1 mm. The scanning width was 50 mm and the axis of ray was vertical to the bone defect surface. The system software

was used to reconstruct 3D images. The upper and lower threshold values for bone were 255 and 85 grey. Because the initial bone defect was round in 5 mm diameter, the region of interest (ROI) was selected to reflect the initial shape. The ROI of each sample was analyzed in bone volume (BV) and bone mineral density (BMD).

Histological staining: Following micro-CT testing, samples were decalcified and dehydrated in a graded series of ethanol. Then samples were embedded in paraffin and cut into 5 μ m sections from the center area of the bony defects. For histological staining, the sections were stained with hematoxylin and eosin (H&E) and then were evaluated by a microscope (Axiovert 40 CFL, Zeiss, Germany).

Statistical analysis

All quantitative data were expressed as mean \pm standard deviation. Comparisons of the data between the groups over time were performed by ANOVA tests with Tukey's post hoc test. Statistical significance was noted at $P < 0.05$.

Results

Characterization of Sr-SFMs

The Sr-SFMs were prepared by electrospinning SF solution with different content of SrCl. The morphology was observed by SEM and fiber diameter was also measured. SEM images in **Figure 2** showed a nanofibrous structure and a morphological change from wire to belt-like morphology. A few strontium chloride nanoparticles were also observed inlaid in the surface of Sr-loaded SFMs. Meanwhile, with the increase of Sr contents, the diameter of nanofibers increased. The average nanofibrous diameter of Sr-SFMs (0, 1, 5 and 10%) were 230 \pm 62 nm, 525 \pm 150 nm, 701 \pm 143 nm and 824 \pm 381 nm respectively ($P < 0.05$).

The XRD analysis of Sr-SFMs was showed in **Figure 3A**. When Sr was introduced into the SFMs in the form of strontium chloride, no additional phase was detected compared to the pure SFMs regardless of the content of strontium chloride. The XPS spectra were shown in **Figure 3B**. All Sr-SFMs revealed four separated peaks referred to C1s (285eV), N1s (403eV),

Strontium-loaded silk fibroin guided bone regeneration

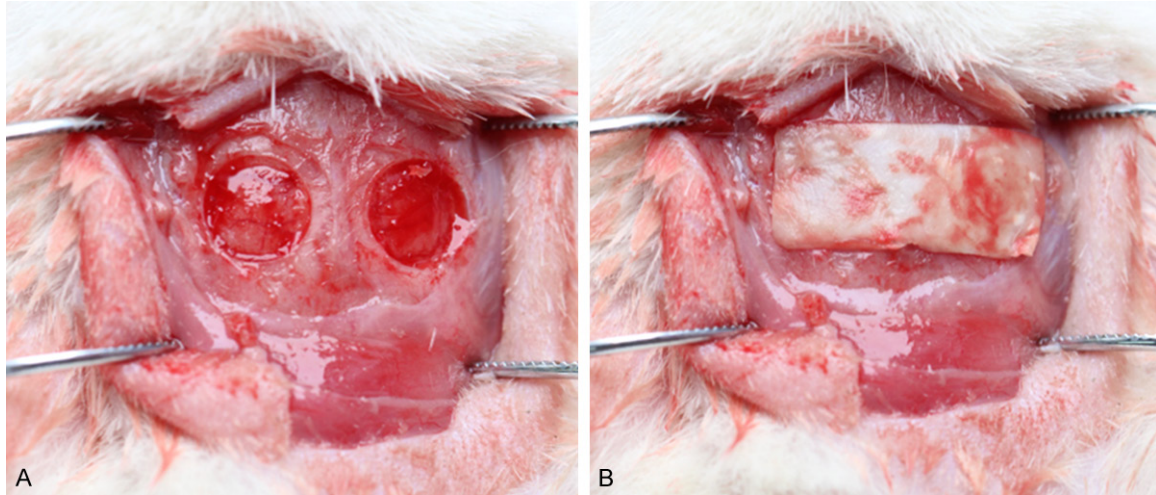


Figure 1. The establishment of rat calvarial defect model. A. Before covered with membranes; B. Covered with membranes.

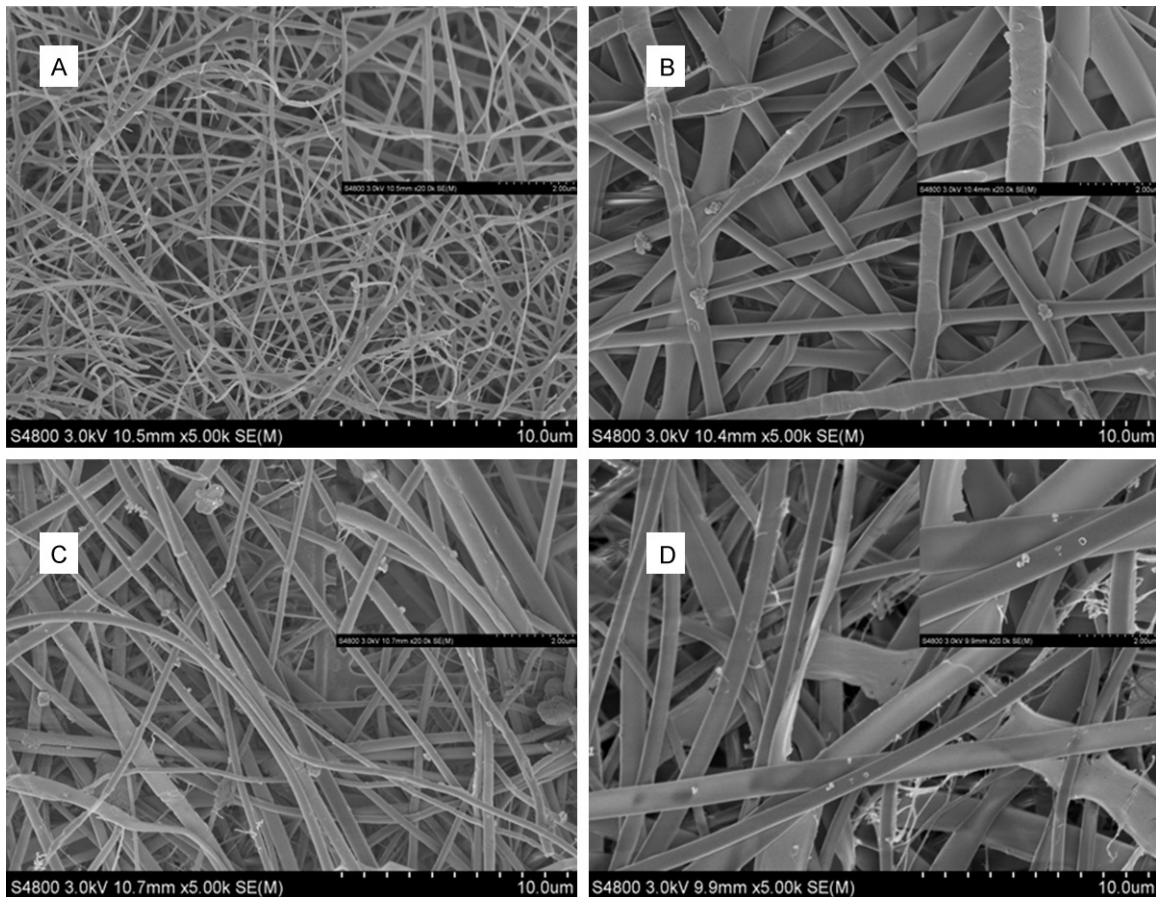


Figure 2. The SEM images of electrospun SF nanofibrous membranes. A. Pure SF, B. 1% Sr-SFM, C. 5% Sr-SFM, D. 10% Sr-SFM.

01s (532eV), and Sr3d (134eV) which is absent in pure SFMs. The relative intensity of the Sr

peak clearly increased as the increase of the initial load of strontium chloride.

Strontium-loaded silk fibroin guided bone regeneration

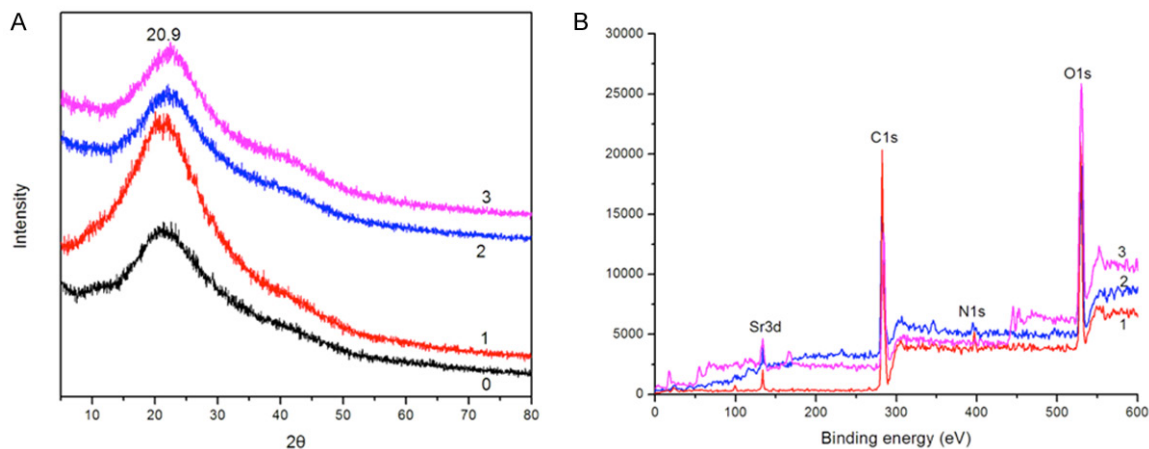


Figure 3. (A) XRD patterns and (B) XPS survey spectra of the samples. (0) pure SF, (1) 1% Sr-SFM, (2) 5% Sr-SFM, (3) 10% Sr-SFM.

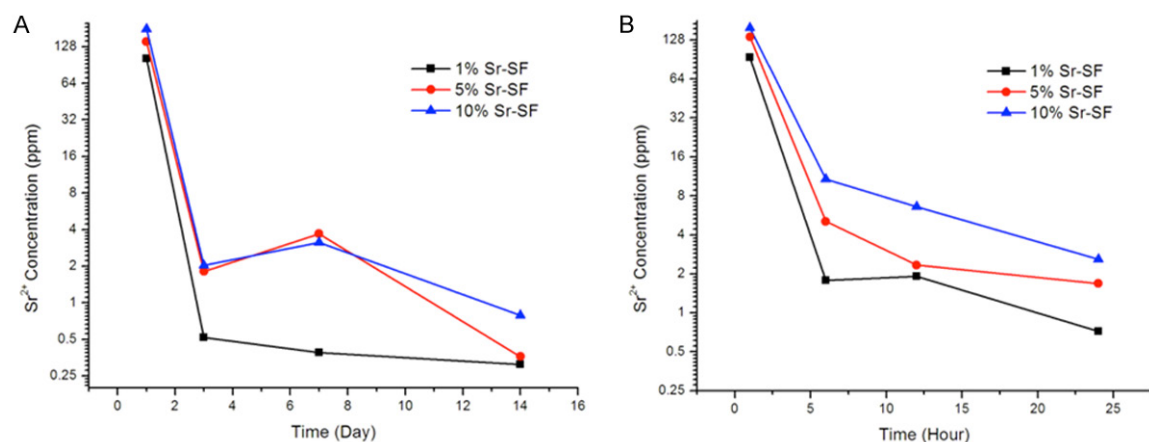


Figure 4. Non-cumulative Sr release time profiles from Sr-SFMs into PBS. A. Release time up to 14 days. B. Release time in first 24 hours.

The release experiments were performed to determine the concentration of Sr released from the Sr-SFMs, as shown in **Figure 4**. For all three groups, a similar release behavior was observed: Sr was continuously released from Sr-SFMs, with an initial burst release during the first 6 hours and slow release rate afterward. After 1 day, the released Sr amounts presented sustainability and slight decline up to 14 days. Except for the burst release after 6 hours, the average Sr amounts released daily from Sr-SFMs (1, 5 and 10%) were 0.094, 0.451, 0.459 ppm, respectively.

Cellular responses to Sr-SFMs *in vitro*

Characterization of BMSCs: In our study, the primary cultured BMSCs from 4-week-old Sprague-Dawley rats were plastic-adherent

and exhibited a fibroblast-like morphology after three passages. Consistent with previous reports [24], these cells were positive for CD73, CD90, and negative for CD34, CD45 when analyzed by FACScan flow cytometry (**Figure 5**).

Morphology and proliferation of BMSCs on Sr-SFMs: The morphology of BMSCs cultured on Sr-SFMs at 1 and 7 days was observed by SEM. After 1 day, BMSCs attached to the Sr-SFMs, and presented well spread morphology along or across the nanofiber. After 7 days, the cell numbers had significantly increased, and formed a cell monolayer almost covered film surface. In addition, the number of BMSCs attaching on the Sr-SFMs was significantly higher than on the the pure SFM based on the SEM observation (**Figure 6**).

Strontium-loaded silk fibroin guided bone regeneration

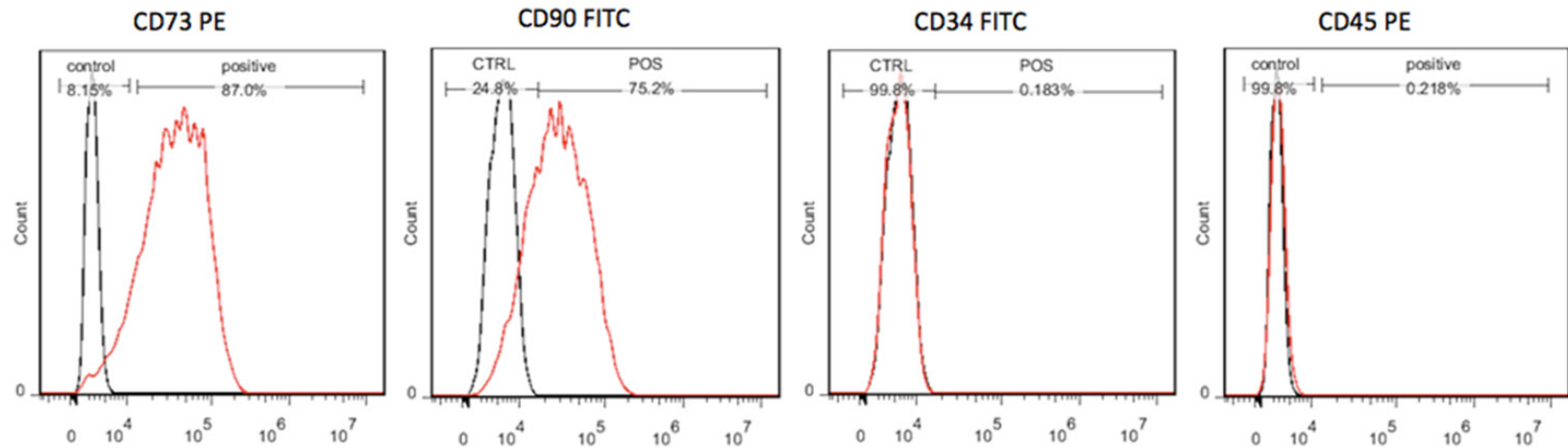


Figure 5. Phenotypic characterization of BMSCs analyzed by flow cytometry.

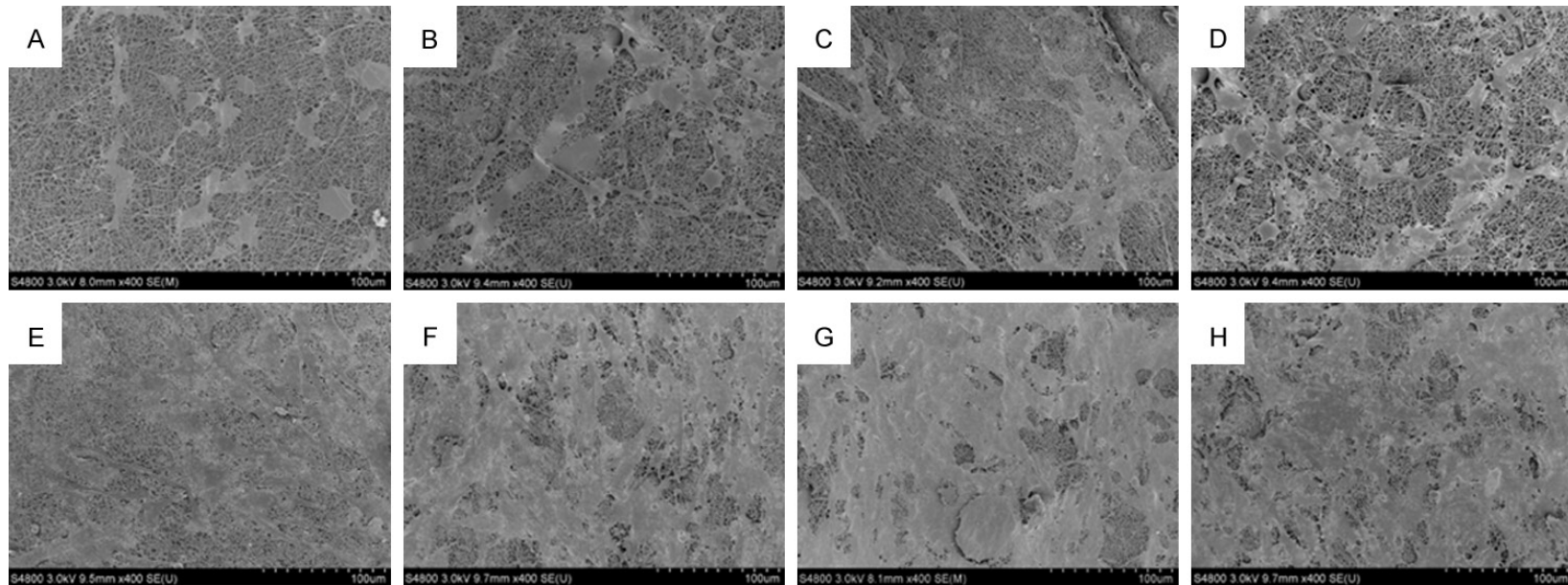


Figure 6. The morphology of BMSCs cultured on membranes. A. Pure SF after 1 day, B. 1% Sr-SFM after 1 day, C. 5% Sr-SFM after 1 day, D. 10% Sr-SFM after 1 day, E. Pure SF after 7 days, F. 1% Sr-SFM after 7 days, G. 5% Sr-SFM after 7 days, H. 10% Sr-SFM after 7 days.

Strontium-loaded silk fibroin guided bone regeneration

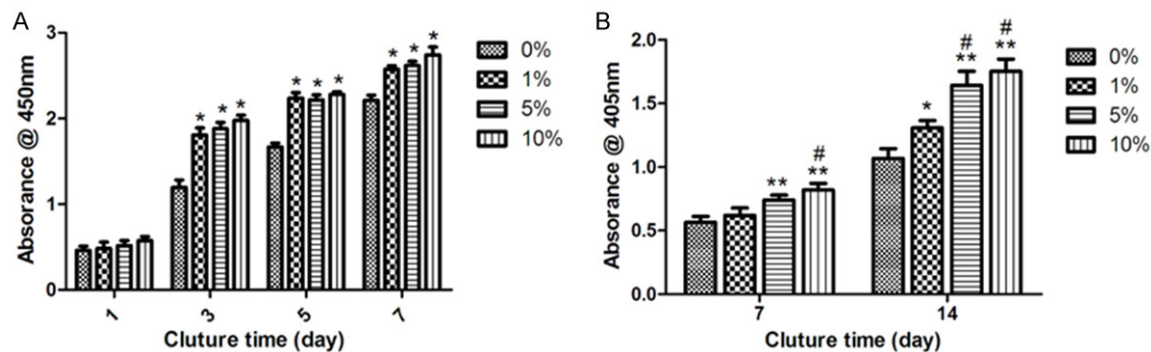


Figure 7. The effect of Sr in SF membranes on the proliferation (A) and ALP activity (B) of BMSCs. Significant difference between the control group and other groups was marked with *P<0.05, **P<0.01. Significant difference between the 1% Sr-SFM group and other Sr-SFM groups was marked with #P<0.05.

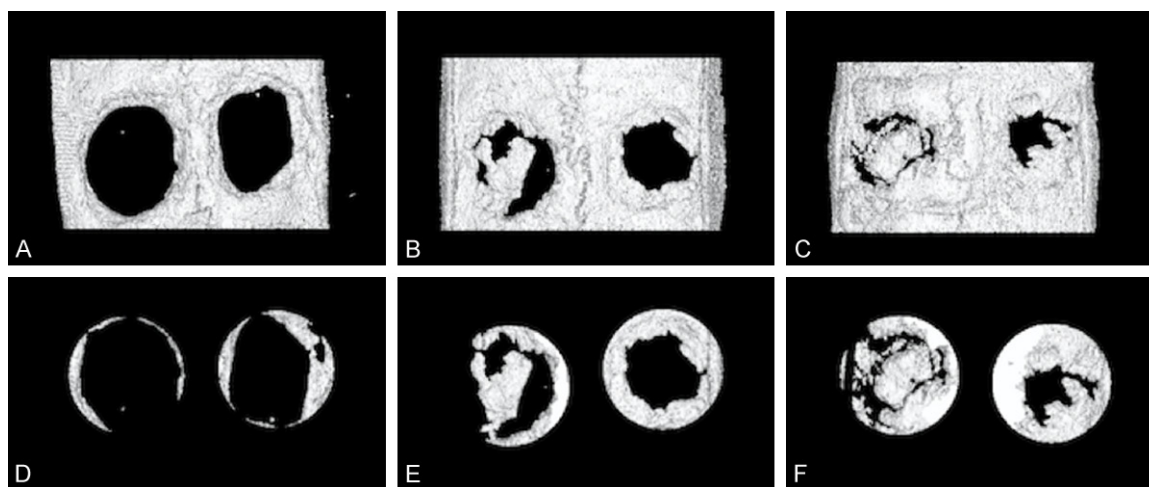


Figure 8. The micro-CT reconstruction images of bone defects at 6 weeks postoperatively. (A) Control group; (B) Covered with SFM group; (C) Covered with 10% Sr-SFM group; (D) The ROI image of (A); (E) The ROI image of (B); (F) The ROI image of (C).

The proliferation of BMSCs on the Sr-SFMs from day 1 to day 7 evaluated by CCK8 assay was shown in **Figure 7A**. The results further revealed that the cell numbers increased linearly along with the extending of culture time. In addition, the proliferation rates on the Sr-SFMs (1, 5 and 10%) were significantly higher than that on the pure SFM (P<0.05). However, the differences between the Sr-SFM groups were not obvious.

ALP activity: The osteogenic differentiation of BMSCs cultured on Sr-SFMs was evaluated by ALP activity assay. Similar to the cell proliferation results, the ALP activity rose sharply as culture time increased from day 7 to day 14, indicating the osteogenic differentiation of BMSCs. The BMSCs cultured on the Sr-SFMs showed

significantly higher ALP activity than that on the pure SFM (**Figure 7B**). Based on these results in vitro studies, we chose 10% Sr-SFM in the follow-up animal studies.

Guided bone regeneration in vivo

Animal general observation: All rats recovered well from the surgery and remained in good health. There was no significant infection, weight reduction or rejection of the membranes until the end of study.

Micro-CT analysis: Micro-CT analysis images and data were presented in **Figures 8** and **9**. At 6 weeks after surgery, the newly formed bone area in 10% Sr-SFM group was greater than in SFM group and control group. The BV value

Strontium-loaded silk fibroin guided bone regeneration

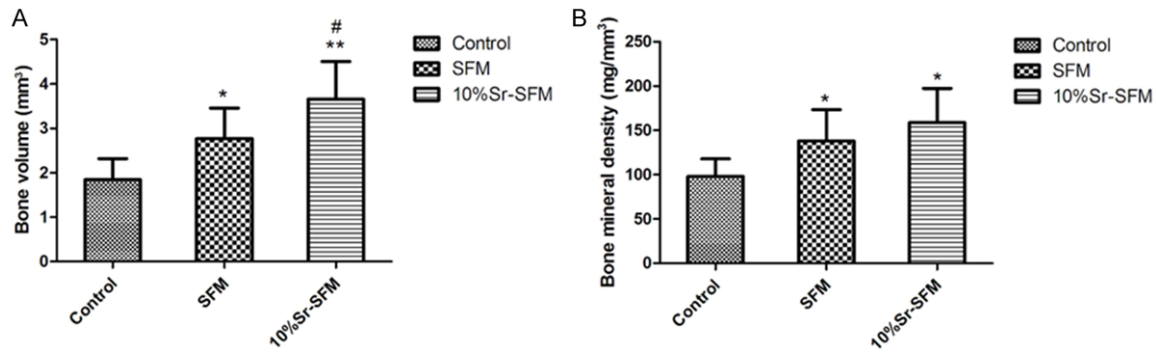


Figure 9. Analysis of new bone formation by micro-CT at 6 weeks postoperatively. A. Bone volume; B. Bone mineral density. Significant difference between the control group and other groups was marked with * $P < 0.05$, ** $P < 0.01$. Significant difference between the SFM group and 10% Sr-SFM group was marked with # $P < 0.05$.

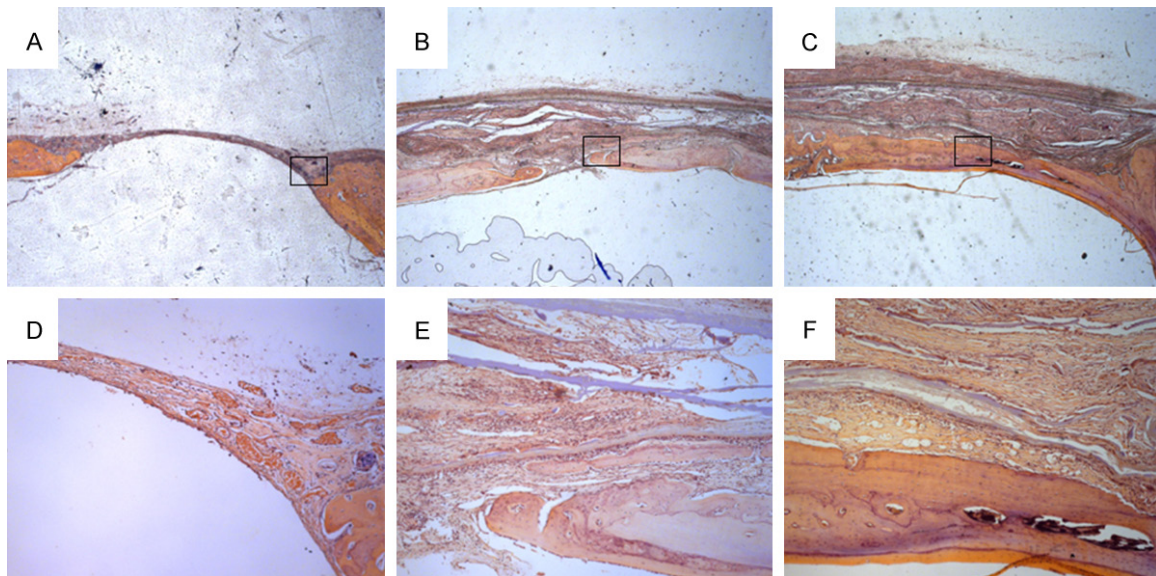


Figure 10. The histological observation of bone defects at 6 weeks postoperatively. (A) Control group (20 \times); (B) Covered with SFM group (20 \times); (C) Covered with 10% Sr-SFM group (20 \times); (D) Higher magnification of selected site of (A) (100 \times); (E) Higher magnification of selected site of (B) (100 \times); (F) Higher magnification of selected site of (C) (100 \times). Arrows: membranes; NB: new bone; OB: original bone.

in 10% Sr-SFM, SFM, control groups was 3.66 ± 0.85 , 2.77 ± 0.69 , and 1.85 ± 0.47 mm³, respectively. More importantly, the BV value in 10% Sr-SFM group was significantly higher than that of the control group ($P < 0.01$) or SFM group ($P < 0.05$). The BMD values in 10% Sr-SFM, SFM, control groups were 158.8 ± 38.5 , 138.1 ± 35.3 , and 98.0 ± 19.7 mg/mm³, respectively. The BMD values in covered groups were significantly higher than in the control group ($P < 0.05$). In addition, the BMD in 10% Sr-SFM group was slightly higher than in SFM group, but there was no statistically difference ($P > 0.05$).

Histological evaluation: H&E staining of rat calvarial defects repaired after 6 weeks were shown in **Figure 10**. In the control group, only small amount of new bone was formed at the defect margins, and the central part of defect was occupied by fibrous connective tissue. In contrast, there were nearly complete closure of the defect in most of the 10% Sr-SFM group and some of the SFM group. Furthermore, new bone and blood vessel formed nicely under the Sr loaded membranes, and a number of woven bones had already been replaced by lamellar bone, whereas a large amount of new bone was still woven bone in the SFM group. In addition,

Strontium-loaded silk fibroin guided bone regeneration

some osteoblast and new bone formation was found occurring in the layers of the membranes.

Discussion

Silk fibroin is an attractive biomaterial and has been used as membranes for GBR because of its desirable properties, such as good biocompatibility, low inflammation and immunogenicity, controllable degradation [6-8]. Recently, electrospun nanofibers have attracted considerable interest in tissue regeneration, including bone reconstruction [25]. SF nanofiber prepared by electrospinning supported MSC attachment, proliferation and ECM deposition, and significantly improved new bone formation at the defect area, demonstrated a potential application for GBR [8]. However, electrospun SF nanofibers usually suffered from the poor tensile strength, which limited its clinical application [26]. Our recent research reported a novel strategy to fabricate SF nanofibrous membrane with significantly improved mechanical properties by preserving silk nanofibril structure during dissolving process [27, 28], which could be an ideal GBR membrane for bone defect repair.

To further enhance the biological activity, strontium chloride was introduced into SFM in consideration of its role in promoting bone formation and remineralization. The SEM observation found that the incorporation of strontium chloride into SF significantly increased the nanofiber diameter under the same electrospinning process. The diameter of pure SF fibers ranged from 200 nm to 350 nm. By contrast, the diameters of Sr-loaded SF fibers were increased to around 800 nm with a belt-like morphology. It was well known that electrospun fiber diameter was proportional to inter fiber spacing, so it was reasonable to expect that the increase in fiber diameter would lead to an increase in inter fiber spacing, thus created an expand and more loose fiber network. The nanofibrous network architectures resulted in high porosity, wide distribution of pore sizes and large surface area to volume ratio, which were favorable factors for cell and tissue in growth, as previous studies [29, 30]. The XRD spectra didn't show diffraction peak of strontium clearly. This result was consistent with Tadier's research, which mainly due to the low crystallinity of strontium

chloride [31]. In addition, the XPS analysis identified and quantified strontium distributed on the surface of SFMs.

Many studies reported association between silk fibroin and drugs as controlled drug release systems [32-35]. The SF materials exhibit drug released behavior dependent on the diffusion of the drug through the SF, the degradation of the SF matrix, or a combination of both [32]. However there was no studies investigated strontium release from Sr-loaded SF. In our ICP-OES study, the SF membranes loaded with different amounts of strontium chloride showed a sustained release profile of Sr^{2+} over at least 14 days. Because of the high solubility and diffusion rate of strontium chloride, a large initial burst release within 6 h was observed, which was similar to a previous report, where strontium chloride was loaded in mineral bone cements [31]. Considering the potential cytotoxicity associated with high concentration of Sr^{2+} , the controlled Sr release system is important for bone tissue engineering application. The effect of Sr dose on osteoblast lineage and mesenchymal stem cells have been described before. Sila-Asna et al. found that a Sr^{2+} concentration between 0.21 and 21.07 ppm in the culture medium enhanced ALP activity and the expression of a key osteoblast transcription factor gene (Cbfa1) in hMSCs [36]. Schumacher M et al. reported a maximum Sr^{2+} concentration ~ 0.1 Mm (8.8 ppm), above which a deleterious effect on proliferation and osteogenic differentiation of hMSCs had to be considered [37]. However, in other studies a stimulation effect of up to 2 mM (176 ppm) Sr^{2+} on ALP expression and bone nodule formation in cultures of MSCs as well as a positive influence of 1 mM Sr^{2+} on cultures of MC3T3 cells had been shown [18, 38]. In our data, the Sr^{2+} dose released from the 10% Sr-SFMs during the first 6 h were close to the maximum Sr^{2+} concentration in culture medium. Meanwhile, except for this initial burst, the Sr^{2+} doses were all in appropriate range, which wouldn't cause any potential cytotoxicity.

Initial cell adhesion is the key step for cell proliferation and differentiation on biomaterials [39]. In our vitro studies, the adhesion and proliferation of MSCs cultured on Sr-SFMs were evaluated by SEM images and CCK-8 assay. From our results, well spread MSCs with a typi-

cal polygonal and flattened morphology were observed on all tested membranes. However, compared to Sr-SFMs, the initial cell adherence was lower on pure SFM and the cell number increased fewer during the culture time. Similar results have been described in previous studies about strontium incorporation other biomaterials. Xue et al. compared sintered SrHA with pure HA ceramic scaffolds and found an improved attachment and higher proliferation of human osteoprecursor cells [40]. Meanwhile, Panzavolta et al. found that Sr incorporation has a slight positive effect on the early adherent cell number [41]. It has been proved that well spread MSCs are inclined to undergoing osteogenesis [42]. The ALP activity is considered as a major early marker of osteogenic differentiation of osteoblast lineage. In this study, the ALP activity of BMSCs on Sr-SFMs was higher than that on pure SFM. The data were consistent with earlier findings that strontium could enhance osteogenic process by increasing ALP expression during induction time [18, 37, 43]. Since Sr overdose may lead to cytotoxicity [44], our in vitro data didn't show any deleterious effect of the Sr release levels and it is likely that the samples releasing higher levels of Sr would be able to observe further increase beneficial effects.

To explore the potential clinical application of Sr-SFM for guided bone regeneration, the rat calvarial defect model was used in vivo study. A critical defect size of 5 mm in rat calvarial has been defined as the smallest bone defect which does not heal spontaneously in its lifetime [45]. In present study, the Micro-CT and histology results indicated that the Sr incorporated with SF could enhance bone regeneration as compared to pure SF material. The mechanical stability of GBR membranes is an essential factor for the clinical success of GBR therapy. Moreover, the extent and rate of degradation may influence the new bone formation by changing the mechanical stability of the membranes used [46]. In our previous studies, we reported a new strategy to fabricate silk fibroin nanofibers with improved mechanical properties by dissolving silk in CaCl_2 -FA, which could provide remarkable mechanical stability compared to other commercial materials [27, 47]. Thus, in histological study, no collapse or distortion of membranes was observed at the 6 weeks. Meanwhile, partially degradation from the inte-

rior parts of the membranes was found and they were separated into layers with different thickness. However, the surface of the membranes could maintain morphological integrity, which provided the space for bone formation, and prevented invasion of soft tissue. It was interesting to notice that some osteoblast and new bone formed under the separated layers. Therefore, we assumed that the separated layers of the degradative membranes could form as lots of GBR membranes with different thickness, thus increased the new bone regeneration.

As is evident from our Sr release results, a large amount of Sr was released in the first 6 h. A large burst release was often regarded as a negative effect for a long term controlled released system, as it might shorten the release profile, which required more frequent dosing [48]. However, Tadier S et al. suggested that the early released dose of Sr had a determinate role on the cell proliferation [31]. In addition, Ji W et al. considered the large initial burst release was favorable for clinical application, because it was likely to enable local released-dose up to effective threshold within a short time, hence triggering stem/progenitor cell recruitment as well as subsequent tissue regeneration [49]. In relation to further study, it would be interesting to design Sr-SF material with a stable long-term release profile, and compare the burst versus long-term characteristics, in order to investigate which of the two characteristics is more effective for bone tissue regeneration.

Conclusions

We fabricated a novel strontium-loaded silk fibroin nanofibrous membrane by electrospinning process. It provided good biocompatibility, slow strontium ion release, clinical manageability and cost efficiency. With the limitation of this study, long-term research in large animal defect model is required to further assess. Based on present results, the strontium-loaded silk fibroin nanofibrous membrane is an efficient potential candidate as GBR membrane.

Acknowledgements

The study was supported by Science Foundation of The Health Department of Jiangsu Province (JZ201401), and Science and Technology

Strontium-loaded silk fibroin guided bone regeneration

Development Program of Suzhou (SYSD2014-070).

Disclosure of conflict of interest

None.

Address correspondence to: Hongchen Liu, Institute of stomatology, Chinese People Liberation Army General Hospital, Beijing, China. E-mail: liu-hc@301dent.com; Zhendong Wang, Jiangsu Key Laboratory of Oral Diseases, Affiliated Hospital of Stomatology, Nanjing Medical University, Nanjing, China. E-mail: wangzhd74@hotmail.com

References

- [1] Dahlin C, Linde A, Gottlow J, Nyman S. Healing of bone defects by guided tissue regeneration. *Plast Reconstr Surg* 1988; 81: 672-6.
- [2] Bottino MC, Thomas V, Schmidt G, Vohra YK, Chu TM, Kowolik MJ, Janowski GM. Recent advances in the development of GTR/GBR membranes for periodontal regeneration—a materials perspective. *Dent Mater* 2012; 28: 703-21.
- [3] Becker W, Dahlin C, Lekholm U, Bergstrom C, van Steenberghe D, Higuchi K, Becker BE. Five-year evaluation of implants placed at extraction and with dehiscences and fenestration defects augmented with ePTFE membranes: results from a prospective multicenter study. *Clin Implant Dent Relat Res* 1999; 1: 27-32.
- [4] Schwartzmann M. Use of collagen membranes for guided bone regeneration: a review. *Implant Dent* 2000; 9: 63-6.
- [5] Altman GH, Diaz F, Jakuba C, Calabro T, Horan RL, Chen J, Lu H, Richmond J, Kaplan DL. Silk-based biomaterials. *Biomaterials* 2003; 24: 401-16.
- [6] Wray LS, Hu X, Gallego J, Georgakoudi I, Omenetto FG, Schmidt D, Kaplan DL. Effect of processing on silk-based biomaterials: reproducibility and biocompatibility. *J Biomed Mater Res B Appl Biomater* 2011; 99: 89-101.
- [7] Kundu B, Rajkhowa R, Kundu SC, Wang X. Silk fibroin biomaterials for tissue regenerations. *Adv Drug Deliv Rev* 2013; 65: 457-70.
- [8] Kim KH, Jeong L, Park HN, Shin SY, Park WH, Lee SC, Kim TI, Park YJ, Seol YJ, Lee YM, Ku Y, Rhyu IC, Han SB, Chung CP. Biological efficacy of silk fibroin nanofiber membranes for guided bone regeneration. *J Biotechnol* 2005; 120: 327-39.
- [9] Pham QP, Sharma U, Mikos AG. Electrospun poly(epsilon-caprolactone) microfiber and multilayer nanofiber/microfiber scaffolds: characterization of scaffolds and measurement of cellular infiltration. *Biomacromolecules* 2006; 7: 2796-805.
- [10] Yang F, Both SK, Yang X, Walboomers XF, Jansen JA. Development of an electrospun nano-apatite/PCL composite membrane for GTR/GBR application. *Acta Biomater* 2009; 5: 3295-304.
- [11] Lee SW, Kim SG, Song JY, Kweon H, Jo YY, Lee KG, Kang SW, Yang BE. Silk fibroin and 4-hexyl-resorcinol incorporation membrane for guided bone regeneration. *J Craniofac Surg* 2013; 24: 1927-30.
- [12] Zhu H, Wu B, Feng X, Chen J. Preparation and characterization of bioactive mesoporous calcium silicate-silk fibroin composite films. *J Biomed Mater Res B Appl Biomater* 2011; 98: 330-41.
- [13] Jin SH, Kweon H, Park JB, Kim CH. The effects of tetracycline-loaded silk fibroin membrane on proliferation and osteogenic potential of mesenchymal stem cells. *J Surg Res* 2014; 192: e1-9.
- [14] Yu T, Ye J, Wang Y. Preparation and characterization of a novel strontium-containing calcium phosphate cement with the two-step hydration process. *Acta Biomater* 2009; 5: 2717-27.
- [15] Thormann U, Ray S, Sommer U, Elkhassawna T, Rehling T, Hundgeburth M, Henß A, Rohnke M, Janek J, Lips KS, Heiss C, Schlewitz G, Szalay G, Schumacher M, Gelinsky M, Schnetzler R, Alt V. Bone formation induced by strontium modified calcium phosphate cement in critical-size metaphyseal fracture defects in ovariectomized rats. *Biomaterials* 2013; 34: 8589-98.
- [16] Schumacher M, Henss A, Rohnke M, Gelinsky M. A novel and easy-to-prepare strontium(II) modified calcium phosphate bone cement with enhanced mechanical properties. *Acta Biomater* 2013; 9: 7536-44.
- [17] Boanini E, Torricelli P, Gazzano M, Della Bella E, Fini M, Bigi A. Combined effect of strontium and zoledronate on hydroxyapatite structure and bone cell responses. *Biomaterials* 2014; 35: 5619-26.
- [18] Yang F, Yang D, Tu J, Zheng Q, Cai L, Wang L. Strontium enhances osteogenic differentiation of mesenchymal stem cells and in vivo bone formation by activating Wnt/catenin signaling. *Stem Cells* 2011; 29: 981-91.
- [19] Andersen OZ, Offermanns V, Sillassen M, Almtoft KP, Andersen IH, Sorensen S, Jeppesen CS, Kraft DC, Bøttiger J, Rasse M, Kloss F, Foss M. Accelerated bone ingrowth by local delivery of strontium from surface functionalized titanium implants. *Biomaterials* 2013; 34: 5883-90.
- [20] Lin K, Xia L, Li H, Jiang X, Pan H, Xu Y, Lu WW, Zhang Z, Chang J. Enhanced osteoporotic bone

Strontium-loaded silk fibroin guided bone regeneration

- regeneration by strontium-substituted calcium silicate bioactive ceramics. *Biomaterials* 2013; 34: 10028-42.
- [21] Sabareeswaran A, Basu B, Shenoy SJ, Jaffer Z, Saha N, Stamboulis A. Early osseointegration of a strontium containing glass ceramic in a rabbit model. *Biomaterials* 2013; 34: 9278-86.
- [22] Zhao L, Wang H, Huo K, Zhang X, Wang W, Zhang Y, Wu Z, Chu PK. The osteogenic activity of strontium loaded titania nanotube arrays on titanium substrates. *Biomaterials* 2013; 34: 19-29.
- [23] Maniopoulos C, Sodek J, Melcher AH. Bone formation in vitro by stromal cells obtained from bone marrow of young adult rats. *Cell Tissue Res* 1988; 254: 317-30.
- [24] Huang Y, Jia X, Bai K, Gong X, Fan Y. Effect of fluid shear stress on cardiomyogenic differentiation of rat bone marrow mesenchymal stem cells. *Arch Med Res* 2010; 41: 497-505.
- [25] Jang JH, Castano O, Kim HW. Electrospun materials as potential platforms for bone tissue engineering. *Adv Drug Deliv Rev* 2009; 61: 1065-83.
- [26] Seok H, Kim MK, Kim SG, Kweon H. Comparison of silkworm-cocoon-derived silk membranes of two different thicknesses for guided bone regeneration. *J Craniofac Surg* 2014; 25: 2066-9.
- [27] Zhang F, Lu Q, Ming J, Dou H, Liu Z, Zuo B, et al. Silk dissolution and regeneration at the nanofibril scale. *Journal of Materials Chemistry B* 2014; 2: 3879.
- [28] Liu Z, Zhang F, Ming J, Bie S, Li J, Zuo B. Preparation of electrospun silk fibroin nanofibers from solutions containing native silk fibrils. *Journal of Applied Polymer Science* 2015; 132.
- [29] Badylak SF. The extracellular matrix as a scaffold for tissue reconstruction. *Semin Cell Dev Biol* 2002; 13: 377-83.
- [30] Li WJ, Laurencin CT, Caterson EJ, Tuan RS, Ko FK. Electrospun nanofibrous structure: a novel scaffold for tissue engineering. *J Biomed Mater Res* 2002; 60: 613-21.
- [31] Tadier S, Bareille R, Siadous R, Marsan O, Charvillat C, Cazalbou S, Amédée J, Rey C, Combes C. Strontium-loaded mineral bone cements as sustained release systems: Compositions, release properties, and effects on human osteoprogenitor cells. *J Biomed Mater Res B Appl Biomater* 2012; 100: 378-90.
- [32] Pritchard EM, Hu X, Finley V, Kuo CK, Kaplan DL. Effect of silk protein processing on drug delivery from silk films. *Macromol Biosci* 2013; 13: 311-20.
- [33] Diab T, Pritchard EM, Uhrig BA, Boerckel JD, Kaplan DL, Guldberg RE. A silk hydrogel-based delivery system of bone morphogenetic protein for the treatment of large bone defects. *J Mech Behav Biomed Mater* 2012; 11: 123-31.
- [34] Zhang W, Zhu C, Ye D, Xu L, Zhang X, Wu Q, Zhang X, Kaplan DL, Jiang X. Porous silk scaffolds for delivery of growth factors and stem cells to enhance bone regeneration. *PLoS One* 2014; 9: e102371.
- [35] Zhang H, Li LL, Dai FY, Zhang HH, Ni B, Zhou W, Yang X, Wu YZ. Preparation and characterization of silk fibroin as a biomaterial with potential for drug delivery. *J Transl Med* 2012; 10: 117.
- [36] Sila-Asna M, Bunyaratvej A, Maeda S, Kitaguchi H, Bunyaratavej N. Osteoblast differentiation and bone formation gene expression in strontium-inducing bone marrow mesenchymal stem cell. *Kobe J Med Sci* 2007; 53: 25-35.
- [37] Schumacher M, Lode A, Helth A, Gelinsky M. A novel strontium(II)-modified calcium phosphate bone cement stimulates human-bone-marrow-derived mesenchymal stem cell proliferation and osteogenic differentiation in vitro. *Acta Biomater* 2013; 9: 9547-57.
- [38] Barbara A, Delannoy P, Denis BG, Marie PJ. Normal matrix mineralization induced by strontium ranelate in MC3T3-E1 osteogenic cells. *Metabolism* 2004; 53: 532-7.
- [39] Anselme K. Osteoblast adhesion on biomaterials. *Biomaterials* 2000; 21: 667-81.
- [40] Xue W, Moore JL, Hosick HL, Bose S, Bandyopadhyay A, Lu WW, Cheung KM, Luk KD. Osteoprecursor cell response to strontium-containing hydroxyapatite ceramics. *J Biomed Mater Res A* 2006; 79: 804-14.
- [41] Panzavolta S, Torricelli P, Sturba L, Bracci B, Giardino R, Bigi A. Setting properties and in vitro bioactivity of strontium-enriched gelatin-calcium phosphate bone cements. *J Biomed Mater Res A* 2008; 84: 965-72.
- [42] McBeath R, Pirone DM, Nelson CM, Bhadriraju K, Chen CS. Cell shape, cytoskeletal tension, and RhoA regulate stem cell lineage commitment. *Dev Cell* 2004; 6: 483-95.
- [43] Su WT, Wu PS, Huang TY. Osteogenic differentiation of stem cells from human exfoliated deciduous teeth on poly(epsilon-caprolactone) nanofibers containing strontium phosphate. *Mater Sci Eng C Mater Biol Appl* 2015; 46: 427-34.
- [44] Zhang W, Shen Y, Pan H, Lin K, Liu X, Darvell BW, Lu WW, Chang J, Deng L, Wang D, Huang W. Effects of strontium in modified biomaterials. *Acta Biomater* 2011; 7: 800-8.
- [45] Rakhmatia YD, Ayukawa Y, Furuhashi A, Koyano K. Microcomputed tomographic and histomorphometric analyses of novel titanium mesh membranes for guided bone regeneration: a study in rat calvarial defects. *Int J Oral Maxillofac Implants* 2014; 29: 826-35.

Strontium-loaded silk fibroin guided bone regeneration

- [46] Cao Y, Wang B. Biodegradation of silk biomaterials. *Int J Mol Sci* 2009; 10: 1514-24.
- [47] Zhang F, You X, Dou H, Liu Z, Zuo B, Zhang X. Facile Fabrication of Robust Silk Nanofibril Films via Direct Dissolution of Silk in CaCl₂-Formic Acid Solution. *ACS Appl Mater Interfaces* 2015; 7: 3352-61.
- [48] Huang X, Brazel CS. On the importance and mechanisms of burst release in matrix-controlled drug delivery systems. *J Control Release* 2001; 73: 121-36.
- [49] Ji W, Yang F, Ma J, Bouma MJ, Boerman OC, Chen Z, van den Beucken JJ, Jansen JA. Incorporation of stromal cell-derived factor-1alpha in PCL/gelatin electrospun membranes for guided bone regeneration. *Biomaterials* 2013; 34: 735-45.